Molecular-Level Understanding of Protein Adsorption at the Interface between Water and a Strongly Interacting Uncharged Solid Surface

Matthew J. Penna, Milan Mijajlovic, and Mark J. Biggs*

School of Chemical Engineering, The University of Adelaide, Adelaide, Australia, 5005

Ⓢ *Supporting Information*

ABSTRACT: Although protein adsorption on solids is of immense relevance, experimental limitations mean there is still a remarkable lack of understanding of the adsorption mechanism, particularly at a molecular level. By subjecting 240+ molecular dynamics simulations of two peptide/water/ solid surface systems to statistical analysis, a generalized molecular level mechanism for peptide adsorption has been identified for uncharged surfaces that interact strongly with the solution phase. This mechanism is composed of three phases:

(1) biased diffusion of the peptide from the bulk phase toward the surface; (2) anchoring of the peptide to the water/solid interface via interaction of a hydrophilic group with the water adjacent to the surface or a strongly interacting hydrophobic group with the surface; and (3) lockdown of the peptide on the surface via a slow, stepwise and largely sequential adsorption of its residues, which we term 'statistical zippering'. The adsorption mechanism is dictated by the existence of water layers adjacent to the solid and orientational ordering therein. By extending the solid into the solution by ~8 Å and endowing it with a charged character, the water layers ensure the peptide feels the effect of the solid at a range well beyond the dispersion force that arises from it, thus inducing biased diffusion from afar. The charging of the interface also facilitates anchoring of the peptide near the surface via one of its hydrophilic groups, allowing it time it would otherwise not have to rearrange and lockdown. Finally, the slowness of the lockdown process is dictated by the need for the peptide groups to replace adjacent tightly bound interfacial water.
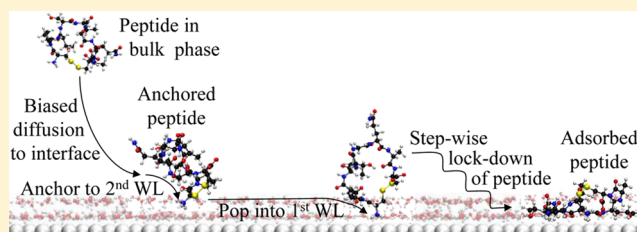
■ INTRODUCTION

Proteins and peptides can be found at liquid/solid interfaces throughout nature, science, medicine, and technology. Proteins play a central role in biomineralization, the process that underpins the formation of bone and other mineralized tissue,[1] and which is now being explored as a means of making synthetic materials with properties as exceptional as those found in nature.[2,3] Nanoparticles introduced into the body are quickly coated by a protein layer[4] that strongly influences their fate and impact—negative or otherwise—on the body. Learning from this, researchers are now functionalizing the surfaces of nanoparticles so as to better target vaccines and image-enhancing nanoparticles while eliminating their toxicity.[5,6] Similarly, surfaces of tissue scaffolds are now being engineered to reduce nonspecific adsorption of the body's proteins, which leads to adverse responses to the scaffold when implanted, while enhancing the binding of cells.[7] Again borrowing from nature, this time the capacity of proteins to naturally form complex functional systems, researchers are actively exploring the use of both synthetic and natural peptides to self-assemble nanostructured materials and systems.[8,9] Adsorption of proteins and peptides on solid surfaces is also relevant to a range of putative biosensor technologies[10−12] and purification of proteins and vaccines.[13,14]

Protein and peptide adsorption at liquid/solid interfaces has been the subject of much experimental investigation since the work of Vroman[15] in the early 1960s. It is now understood that protein adsorption at such interfaces is inevitable except in limited circumstances[16] and that it is largely irreversible except under certain conditions (e.g., the Vroman effect).[15] There is also some understanding of the protein adsorption mechanisms (e.g., Norde,[17] Mermut et al.[18] and Li et al.[19]), but it is largely limited to what could be termed the colloidal scale where molecular-level details are largely absent, and it is still far from complete as demonstrated by the myriad of models that have been proposed for protein adsorption and the debate that still circles around them.[20] Similarly, there is still debate around the origins of bioresistance of solid surfaces,[21,22] with several competing theories, including steric repulsion,[23,24] hydration theory,[25,26] and hybrids of these (e.g., Li et al.[27] and Pasche et al.[28]). These and other examples have led many to comment even within the last year or so that understanding of the mechanism of protein adsorption is still relatively poor,[20,29,30] particularly at the molecular level.[16,31,32]

In the face of limitations in the experimental approach, a number of groups have turned to molecular simulation to
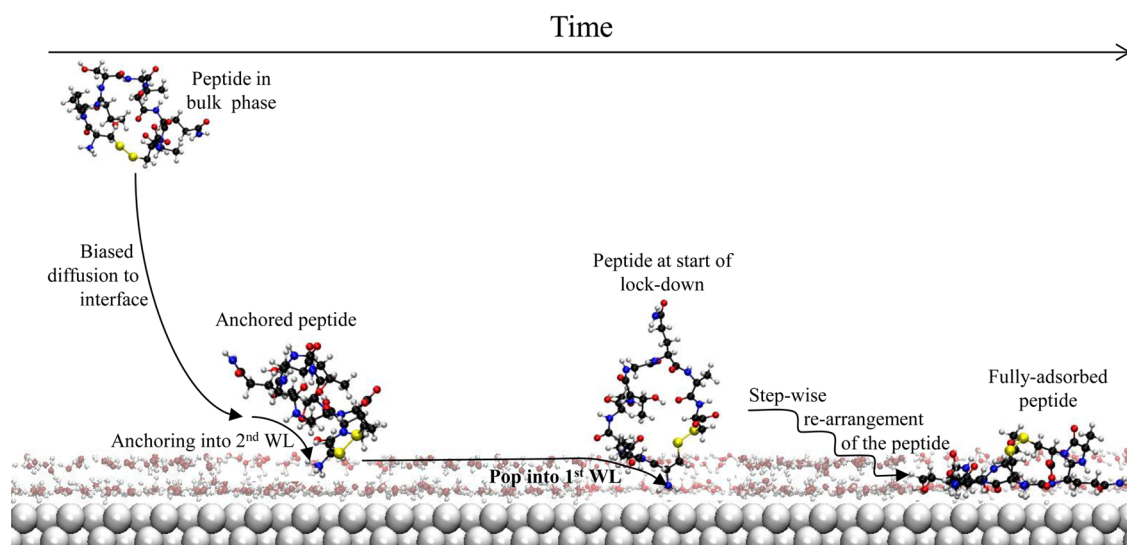
Figure 1. Tentative generic peptide adsorption mechanism identified by Penna and Biggs;[44] see text for description of this mechanism.

provide the missing understanding on peptide and protein adsorption at liquid/solid interfaces (e.g., refs 33−48). All but two of these studies have, however, focused on the adsorbed state without considering the process the peptide or protein undergoes as it moves from the bulk solution far from the solid surface to the adsorbed state. In the earlier of the two studies in which the peptide starts outside the range of the peptide−solid surface interaction, Penna and Biggs[44] identified a putative three-phase adsorption mechanism as illustrated in Figure 1: (1) biased diffusion toward the interface; (2) 'anchoring' of the peptide via a hydrophilic group of the peptide to the second water layer (WL) that occurs adjacent to the solid surface; and finally (3) formation of the fully adsorbed peptide through a ('lockdown') process of stepwise rearrangement of the peptide that is initiated by the anchor group popping into the WL immediately adjacent to the surface. In the second study of this nature, Yu et al.[48] independently present essentially the same process,[49] although they have missed a number of key aspects such as, e.g., the biased nature of the diffusion toward the surface, the existence of the anchoring phase (which is different from their 'anchoring regime'),[49] and the critical role played by hydrogen bonding between the interfacial water and the peptide in this phase.

While both Penna and Biggs[44] and Yu et al.[48] offer up significant new molecular-level insight into the adsorption mechanism, it is not possible to assert the generality of their proposed mechanisms because of the limited number of simulations involved (10 in Penna and Biggs[44] and 5 in Yu et al.[48]) and their focus on a single peptide; is the mechanism in Figure 1 a general one or are there variations? Furthermore, neither study offered up any insight into why biased diffusion toward the solid surface appears to start when the distance between the peptide and the surface exceeds the range of the dispersion interaction between them; was it just happenstance in the few simulations considered or is there another reason based in the physics?

By considering results from over 240 MD simulations of up to 100 ns length in which one of two different peptides adsorb after starting from a distance beyond the range of the peptide−solid surface interaction, we offer up here what we believe is a generalized peptide adsorption mechanism at a molecular level for the case where the interaction between the surface and the

solution above it is strong such as would occur for metal surfaces; as part of this, we address the questions raised above. Following presentation of the mechanism, support for it is drawn from the limited experimental data available as well as other molecular simulation studies. Some implications of the findings presented here are then outlined before conclusions are drawn.

■ METHOD

The conclusions drawn here are based on a detailed consideration of adsorption in two separate peptide/surface systems: (1) SD152, an experimentally identified platinum-binding peptide,[36,50,51] at the interface between pH-neutral water and an uncharged Pt(111) surface; and (2) A3, a similarly identified gold-binding peptide,[52] at the interface between pH-neutral water and an uncharged Au(111) surface (see Supporting Information (SI) for details of how the peptides, water, and surfaces are modeled). The SD152 peptide has a closed loop structure by virtue of a disulfide bond between the cysteine residues at either end of its sequence, which is CPTSTGQAC.[53] The A3 peptide, on the other hand, is linear with a sequence of AYSSGAPPMPPF.[53] As will become clear later in this report, it is important to note that at the neutral pH considered here, the termini of both peptides are charged (i.e., NH_3^+ and COO^-), the residue side chains are all neutral, and they contain a mixture of both hydrophilic (S, T, Q, Y) and hydrophobic (C, P, G, A, F, M) residues. Both peptides also include sulfur-containing residues (C and M) that in isolation can chemically bind to both gold and platinum. There is, however, experimental evidence that suggests this does not occur for either peptide considered here: (1) in the case of the A3 peptide, it has been observed to adsorb less effectively on gold when its sole tyrosine residue (Y2) is replaced by serine, indicating chemical binding to gold by the methionine (M9) residue is unlikely; and (2) for SD152, desorption has been observed[51] suggesting chemical bonding between the cysteine residues and platinum does not occur in all cases if at all, possibly due to steric hindrance.[36]
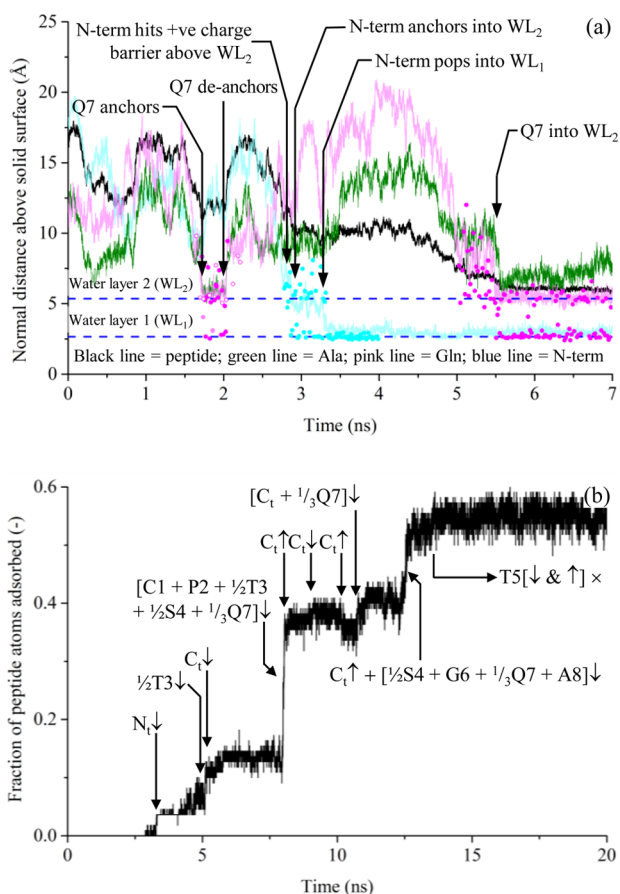
In order to establish the generality of the adsorption mechanism outlined below, 159 and 84 independent molecular dynamics (MD) simulations were undertaken for the SD152 and A3 peptide systems, respectively, as outlined in the SI. Briefly, however, each simulation involved random insertion of a peptide into the water at a distance well beyond the cutoff range of the peptide−solid surface interaction, which was 12 Å. The water/solid system into which the peptide was inserted was at equilibrium at 298 K and 1 atm, and the peptide structure was extracted from a separate simulation of the peptide in bulk water at the same conditions. The water molecules overlapping

the peptide were removed, and the system relaxed to a local energy minimum before being gradually heated up to 298 K. Production simulations were then run for periods ranging from 20 to 100 ns depending on the fate of the peptide.

■ RESULTS

All 165 of the SD152 and 84 of the A3 simulations undertaken for this report adhered to the mechanism of Figure 1. The larger number of simulations has meant, however, that we have been able to detect some important variations on this mechanism and gain substantial new insight. To assist in drawing these out, we consider in the following sections the exemplar trajectory shown in Figure 2, a signposted movie of which is available in the SI.

Biased Diffusion Phase. It can be seen early in the exemplar simulation in Figure 2 that the (SD152) peptide moves toward the surface despite the groups nearest to the surface, Gln(7) and Ala(8), initially being outside the cutoff

range of the dispersion interaction explicitly included between the peptide and the solid surface (i.e., beyond 12 Å). This was observed to occur in all the simulations at some point, confirming our earlier observation of biased diffusion from the bulk phase to the interface prior to adsorption.[44] Consideration of the velocity components of the peptide in this phase averaged over a large number of simulations (see the SI) reveals that the components parallel to the surface are statistically zero, while that normal to the surface is clearly not (see Table S2), confirming that biased diffusion occurs toward the solid surface.

The fact that biased diffusion was observed in all the simulations strongly suggests it is more than happenstance; there appears to be another, longer ranged, force at play between the surface and peptide. Figure 3 reveals the origin of
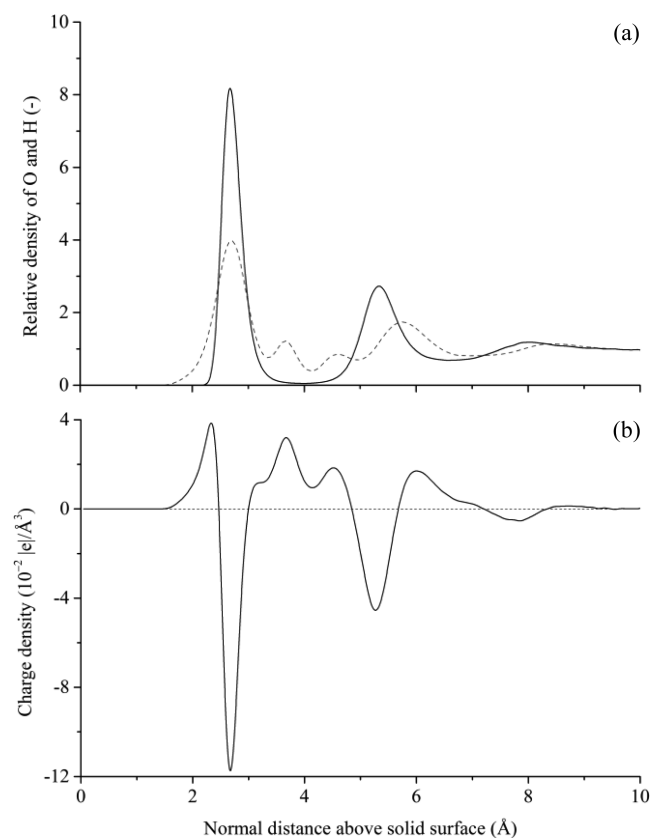
Figure 3. Variation with normal distance above the platinum surface of: (a) relative density of the oxygen (solid line) and hydrogen (broken line) in the water and (b) charge. The profiles for the gold surface (not shown) are very similar.

Figure 2. Trajectory of one of the SD152 MD simulations, presented here as an exemplar: (a) from the start up to somewhat beyond initiation of the lockdown phase, the time variation of the normal distance of the center of mass of key parts of the peptide in this simulation and (b) from the initiation of the lockdown phase to the end of the simulation, the time variation of the fraction of peptide atoms in direct contact with the solid surface (i.e., sitting in or below WL1). In (a) the positions of select water molecules that formed hydrogen bonds with hydrophilic groups of the peptide prior to and just after their lockdown are shown as dots of the same color as the trajectory lines of the groups. In (b) the point where groups pop down on to the surface (↓) and off (↑) are indicated where the Thr(5) residue pops on and off continuously beyond 13 ns and Cys(9) never adsorbs.

this longer-ranged force that induces the biased diffusion. In part, the origin is the layering of the water molecules adjacent to the solid surface as revealed in Figure 3a, which has the effect of projecting the solid surface around 8 Å into the water, augmented by the water layering around the peptide (see Figure S2). More importantly, however, is the orientational ordering of the water adjacent to the solid surface, which is revealed in Figure 3a by the multiple peaks in the hydrogen atom density profile and its difference from that of the oxygen atoms. Because the hydrogen and oxygen atoms carry partial charges of opposite sign, this orientational ordering means the solid surface is endowed with charged layers that in effect brings long-range electrostatic interactions into play between the peptide and the solid surface.

Anchoring Phase. We now turn to the anchoring phase where the peptide engages in a sustained way with the second surface-bound water layer as illustrated in Figure 1. Unlike in our earlier more limited study,[44] it is clear from the work reported here that anchoring is a reversible process: the peptide comes adrift sometime after anchoring in around 23% and 31% of the SD152 and A3 simulations, respectively. This scenario is seen in the exemplar trajectory of Figure 2 where the Gln(7) residue initially anchors the peptide to the interface at around 1.75 ns into the simulation (the Ala(8) residue is entrained with it; see below for further commentary on this) before it detaches again at around 2 ns. In such cases, a second or, occasionally, a third (2 for SD152, 10 for A3), fourth (3 for A3), or even fifth (2 for A3) anchoring event is required before initiation of lockdown goes on to occur.

Our previous more limited study[44] suggested that anchoring occurs by the formation of hydrogen bonds between polar parts of the peptide and the surface-bound water layers seen in Figure 3a. Figure 4a, which attributes the anchoring events seen in the SD152 simulations to its residue side chains and termini, certainly supports the notion that polar parts of a peptide play an important role in anchoring. The side chain of its Gln(7) residue alone accounts for around 31% of all anchoring events, more than three times that of any other group, while a further 40% of the total is split between the other polar residues (3 of) and charged termini.

Counter to our prior more limited study,[44] Figure 4 also indicates the side chains of some of the nonpolar residues of SD152 possess not insignificant anchoring propensities. However, in around 75% (i.e., 12) of the 16 cases where Ala(8) is the 'anchor', the polar side chain of its adjacent Gln(7) residue or, occasionally, its nearby negatively charged C-term are seen to enter the second water layer on average only 41 ps later. Similarly, the nearby charged termini accompany[54] the side chains of both cysteine residues 10 of the 14 times they act as an anchor, while the neighboring polar threonine residues accompany[54] Pro(2) and Gly(6) 33% and 100%, respectively, of the time, they act as anchors. If we combine these events with the ~71% directly linked to hydrophilic groups, such groups play a role in more than 87% of the anchoring events seen for SD152 despite accounting for only ~55% of its makeup. This clearly indicates hydrophilic groups and their interaction with the interfacial water are indeed critical in the anchoring phase of this peptide.

The anchoring statistics for the A3 peptide, which are shown in Figure 4b, tell a not dissimilar story to that of SD152. For example, if the nonpolar anchors accompanied by hydrophilic group[54] are included, around 69% of all anchoring events involve hydrophilic groups despite making up only ~35% of the peptide. There are, however, two notable additional elements to the story here. As Figure 4b shows, the anchoring propensities of the Phe(12) and Met(9) side chains are also comparable to those of the hydrophilic groups despite being hydrophobic. Even though ~26% of the anchoring events of the former involve accompanying hydrophilic groups,[54] it is clear that both these residues possess some anchor-endowing characteristic that the other hydrophobic groups considered here do not. The origin of Met's higher propensity can be found in the strength of the dispersion interaction that arises from its sulfur atom, which is some ~2.5 times stronger than that of a single carbon atom. In the case of Phe, on the other hand, a similar level of dispersion energy arises from the six 'closely packed' carbon atoms of the benzyl ring; this suggests that amino acids with ring-containing side chains (excluding Pro) may also serve as good anchors.

Comparison of Figure 4a with 4b also reveals the anchoring propensity of SD152's C-term (8.9%) is almost twice that of A3's C-term (4.8%). The like (negative) charge of the C-term and the second water layer (see Figure 3b) suggests the SD152 propensity, which is comparable to polar residues, is counterintuitive. However, analysis reveals that anchoring by the SD152's C-term is often accompanied by the side chain of the nearby Gln(7) residue whose anchoring frequency (~31%) is by far the highest of all groups considered here. Converse to this C-term behavior, the anchoring propensity of A3's N-term (12.2%) is nearly three times that of its counterpart in SD152 (4.7%). This propensity of A3's N-term, which is comparable to polar residues, is in keeping with its positive charge being attracted to and retained by the net negative charge of the second water layer (see Figure 3b). The reason for the lower than expected frequency for SD152's N-term is, on the other hand, less clear, but this could possibly arise from one or both of the following: (1) steric effects caused by the adjacent disulfide bonded Cys residues, which are almost always accompanied by one of the termini when acting as an anchor (see Figure 4a), or (2) the adjacency of the negatively charged C-term. Whatever the origin of the contrary anchoring behavior
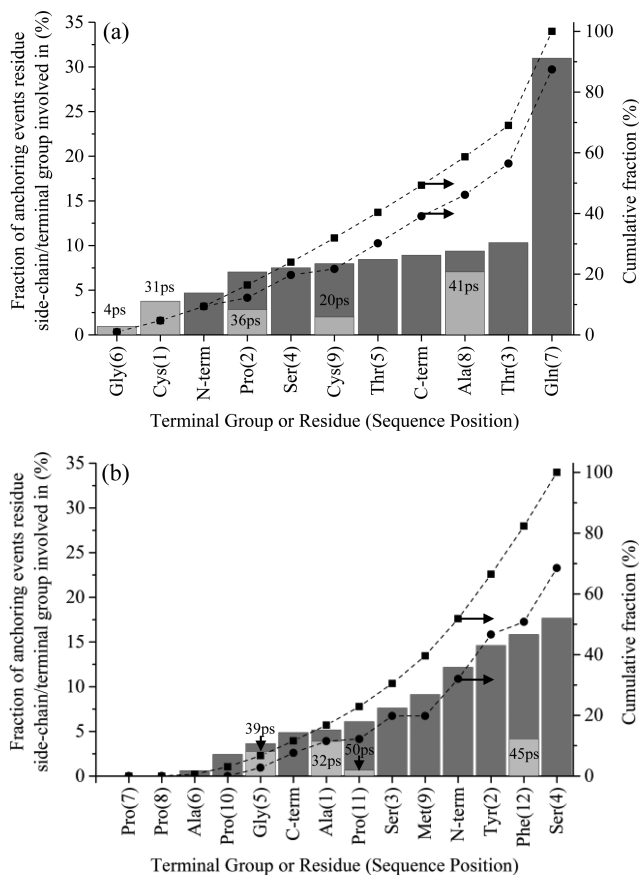
Figure 4. Fraction of anchoring events for terminal/residue side chain groups of: (a) SD152 and (b) A3. There are 213 and 122 anchoring events, respectively. The groups are shown left to right in increasing fraction. The nonpolar group bars are split: where the group is accompanied (54) by a hydrophilic group (light gray with average time to accompaniment shown in ps) or not. The cumulative fraction of net (■) and hydrophilic group-associated events (●) are also shown.

of the termini seen here, it appears their anchoring propensities are dependent on the nature of their adjacent groups.

Lockdown Phase. Lockdown is the process whereby the anchored peptide gradually rearranges itself so as its groups can first enter the second surface-bound water layer and, finally, the water layer immediately adjacent to the solid surface where it binds. Insertion of a peptide group into the second of the surface-bound water layers is rapid (e.g., average time of transition from the weak third water layer at $z \approx 8$ Å to the second water layer is 70 ps for SD152) due to the high rate of transfer of water molecules between the layer and the bulk. Insertion of a peptide group into the surface-bound water layers, on the other hand, is far slower as it requires the formation of cavities in the tightly bound water layer adjacent to the group (see Figure 5 for SD152 and Figure S3 for A3).
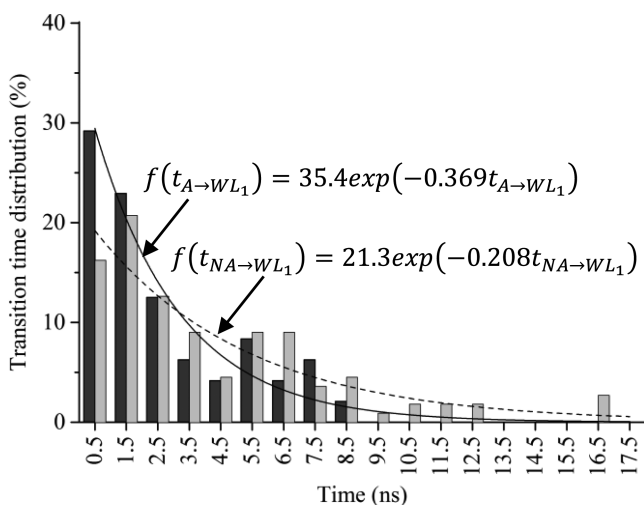
Figure 5. Distribution of the time for SD152's anchor groups (dark gray bars = statistics from the simulations; line = exponential fit) and nonanchor groups (light gray bars = statistics from the simulations; broken line = exponential fit) to transition from the second water layer into the water layer immediately adjacent to the solid surface when initiating lock-down, $t_{A \to WL_1}$ and $t_{NA \to WL_1}$, respectively. There are 165 lockdown initiation events net. The counterpart of this figure for A3 is shown in Figure S3.

This slow rate makes stark the criticality of anchoring: without it, peptide adsorption would be virtually impossible for strongly interacting surfaces such as that considered here.

The need for the anchored peptide to rearrange itself and then wait until it can insert its groups into the water layer immediately adjacent to the solid surface means the lockdown process is always stepwise and lengthy (10+ ns) as illustrated in the exemplar trajectory of Figure 2b. In the case of this trajectory, it is initiated when the positively charged N-term, which anchors the peptide to the interface from around 3 ns, passes into the first water layer at around 3.5 ns. A good fraction of the polar Thr(3) residue follows at around 5 ns trailed quickly by the negatively charged C-term. Much of the peptide between Cys(1) and Ser(4) inclusive go on to adsorb at around 8 ns along with part of the Gln(7) residue; this coadsorption of the glutamine with Cys(1)-Ser(4) reflects the length of the former's side chain. The remainder of the Gln(7) residue adsorbs in two further steps, the first at around 11 ns and the last at 13 ns along with the rest of the Ser(4) residue and the two most hydrophobic residues of the peptide, Gly(6)
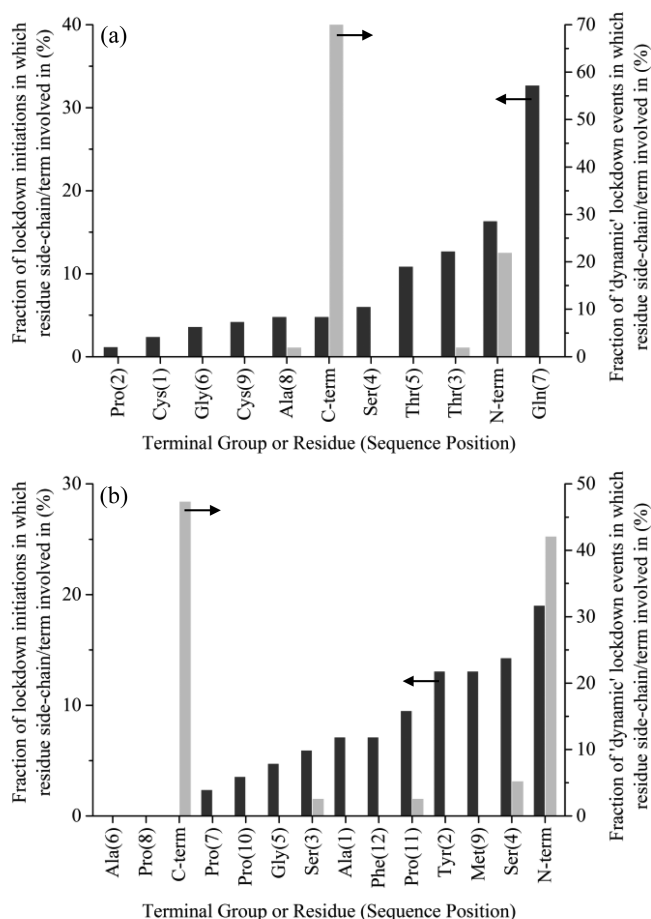
and Ala(8). Beyond this point, the negatively charged C-term adsorbs and desorbs multiple times before finally desorbing at around 13 ns; we will return to the origin of this behavior below along with the reason as to why the associated Cys(9) residue is not seen to adsorb here despite its hydrophobic character providing some driving force to do so. Like the C-term, the Thr(5) residue also oscillates between the adsorbed and desorbed state, in this case due to steric effects.

Intuitively one might expect the anchor to often be the first to pop into the water layer immediately adjacent to the surface and, thereby, initiate lockdown as seen in the exemplar trajectory. Certainly our more limited prior study[44] suggested this was the case. The study here, however, shows this in fact only occurs in ∼26% of the SD152 simulations. This perhaps surprisingly modest rate for the anchor to initiate lockdown, which also prevails for the A3 peptide (34%), reflects the fact that the time for this transition and the alternative of another group initiating lockdown is characterized by overlapping exponential distributions as seen in Figure 5. Comparison of this figure with its counterpart for A3 (see Figure S3) shows that the time scales for the transition from the second to first water layer for both peptides are similar despite their very different natures, further reinforcing the critical role played by the structured water at the solid surface over the nature of the surface itself.

It is of interest to understand what groups if any have some preference for initiating lockdown. Figure 6a indicates that such a preference is indeed seen for the hydrophilic groups of SD152, with around 84% of the lockdown initiation events involving them despite only accounting for ∼55% of the peptide. In the case of A3, the hydrophilic groups initiate lockdown around 54% of the time, Figure 6b, despite only accounting for 35% of the peptide. Akin to anchoring, this bias toward hydrophilic groups initiating lockdown comes from their capacity to form energetically favorable hydrogen bonds with the high density water layer immediately adjacent to the solid surface. The disproportionately high fraction seen for SD152's Gln(7) side chain reflects its two hydrogen-bond-forming groups, which see no bias one way or the other. The strongly interacting sulfur in the Met(9) also appears to endow its side chain with a lockdown initiation propensity that is comparable to that of hydrophilic groups. The ring-containing side chain of Phe(12) on the other hand appears to initiate lockdown somewhat less than Met despite having a similar interaction energy as its sulfur, possibly due to its greater bulk and lesser flexibility requiring a larger water cavity to exist before it can lockdown.

Figure 6 further shows that the N-term is a well-favored group for initiating lockdown in both peptides (∼16% and ∼19% for SD152 and A3, respectively), reflecting the strong attraction that arises between its positive charge and the negative charge associated with the water layer adjacent to the solid surface (see Figure 3). The C-term, on the other hand, is poorly favored (∼5% for SD152, and not at all for A3) in this phase of the adsorption process due to its charge being the same as the water layer adjacent to the surface. This group, instead, prefers to sit in the relatively low density, positively charged region between the two water layers.

Finally, Figure 6 also reveals that both charged terminal groups experience in a significant way what we term 'dynamic' lockdown events where they repeatedly pop in and out of the first water layer as seen for the C-term in the exemplar trajectory, Figure 2b. This arises from thermal fluctuations

$$Prob = 118.3 \exp(-0.765[dist])$$

Figure 7. Probability of a group following the lockdown initiator into the adsorbed state as a function of its 'distance' from the initiator (in residues) for SD152. The statistics derived from the ensemble of simulations are shown as bars and the fit as a broken line with points. The total number of events are 155. The counterpart of this figure for A3 is shown in Figure S4.

Table 1. Self-Diffusion Coefficients of the Peptides in the Bulk Phase and When at the Water/Solid Interface[a]

	self-diffusion coefficient ($10-8$ cm^2/s)	
phase/peptide	SD152	A3
bulk	154.3	90.0
anchored	52.4	55.3
lockdown start	24.0	29.5
over lockdown	3.2	5.9

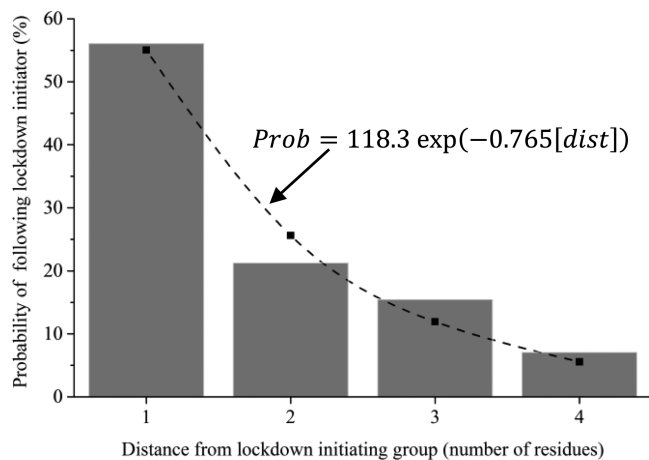[a]See Figure S6 for associated MSD data.

Figure 6. Fraction of stable (dark gray bars) and 'dynamic' (light gray bars) lockdown initiation events for the terminal/residue side chain groups for: (a) SD152 and (b) A3. There are 165 and 84 stable and 50 and 38 dynamic lockdown initiation events for the peptides, respectively.

taking the charged terminal groups into regions of like-charge from which they are ejected soon after back into more favored regions. In this way, the negatively charged C-term fluctuates between the positively charged (but relatively low-density, Figure 3a) region between the water layers and the disfavored first and second water layers, whereas the positively charged N-term behaves conversely.

While hydrophilic groups have a far greater propensity to initiate lockdown, Figure 7 and its counterpart for A3 (Figure S4) shows that the probability of a group being the second to lockdown is exponentially related to the distance from the initial group, with no apparent role being played by the nature of the group (i.e., polar, nonpolar, charged). Analysis of the third group to lockdown reveals a similar exponential relationship to the groups already locked down (see Figure S5), suggesting this is likely to prevail throughout the lockdown process. We, therefore, term this process statistical zippering.

Surface Diffusion during the Adsorption Process. Table 1 shows that the diffusion rate of the anchored peptide across the surface is around ~30% and ~60% of that in the bulk phase for SD152 and A3, respectively. The table further shows that this rate roughly halves again at the onset of lockdown and diminishes rapidly thereafter as the degree of lockdown increases. These results suggest that any significant diffusion of the peptides at the water/solid interface is only likely to

occur between peptide anchoring and initiation of lockdown. Comparison of the MSD plots for the anchored state (see Figure S6) with the average time between anchoring and initiation of lockdown (4.5 and 2.25 for SD152 and A3, respectively) suggests that peptides will diffuse between 10 and 20 Å across the surface before lockdown effectively halts any further significant diffusion.

■ DISCUSSION

Despite the significant differences between the SD152 and A3 peptides, the study reported here clearly demonstrates their adsorption at the interface between water and a strongly interacting surface is well described by the mechanism outlined in Figure 1. Moreover, while there is some quantitative difference between the statistics that characterize the adsorption of each peptide, the trends are essentially identical where one-to-one comparison can be made.

As already indicated in the Introduction, significant limitations with the experimental approach makes it virtually impossible to quantitatively validate the results presented here. However, the results are qualitatively not inconsistent with the limited experimental data available for the peptides considered here. For example, Slocik et al.[52] observed strong physical adsorption between A3 and gold nanoparticles. Similar strong adsorption has also been observed for SD152 on platinum,[50] with only modest desorption occurring upon removal of the peptide supply[51] indicating the adsorption is strong. A link between this slight desorption observed by Seker et al.[51] and

the deanchoring of peptides observed here may also be posited alongside other possible processes.

The results here are also consistent with those of the two earlier more limited studies concerned with following adsorption from the bulk phase through to full adsorption.[44,48] For example, like Yu et al.,[48] we have found that the Phe(12), Tyr(2), and Met(9) residues of the A3 peptide have a high propensity to initiate lockdown, and its Ser(4) residue initiates lockdown far more often than the other serine residue of the peptide. We also observe along with Yu et al.[48] that the negatively charged C-term is disfavored for initiation of lockdown in either peptide. The reason for this behavior is the strong negative charge associated with the first water layer that arises from the orientational structuring of the interfacial water (cf. Figure 3).

Moving beyond the few molecular simulation studies specifically concerned with following the entire adsorption process, there is also independent support for some of the findings presented here. In MD simulations of the 184 residue FibronectinIII modules 9 and 10 initially placed 8 Å from a gold surface, Hoefling et al.[47] observed more rapid than expected diffusion toward the surface as we do here. They did not offer up a reason for this more rapid diffusion, but our results here suggest this may represent 'biased diffusion' caused by the charged layers at the surface arising from the orientational ordering of the interfacial water. This orientational ordering of the water at the solid surface and its importance in the adsorption process, in particular with regards what we term anchoring, has also been highlighted by Skelton et al.[39] for a small peptide on a rutile titania surface. Finally, although a very different peptide (a rigid β-sheet), Hoefling et al.[47] also observed lockdown occurred via a zippering process similar to what we have observed here.

It is of interest to also consider the impact of the potential models used for the peptide, water, and surface. Given the similar functional forms of the various biomolecular potential models (e.g., Amber, CHARMM, Gromos, CVFF) and the fact that they seek to emulate hydrophilic and hydrophobic character of residues and all that emerges from this that is important here, the fundamentals of the mechanism reported here are unlikely to be affected by which of these potentials is used. Similarly, as illustrated by the results of Schravendijk et al.,[55] the fundamentals of the mechanism observed here will not change with any of the realistic water models used (i.e., any 3−5 point charge models) as they all possess the essential features necessary for water structuring at the interface and associated charged layering, namely: (1) the capacity to form hydrogen bonding and, thus, rotational ordering under the strong binding of the surface and (2) distributed positive and negative charges. In the case of metal surfaces, on the other hand, electron polarization is known to occur in the presence of charges, something not explicitly captured in the Lennard-Jones representation used here and more widely by others. We, therefore, duplicated on a smaller scale the A3 study using the polarizable gold surface model of Corni and co-workers[56,57] and, as summarized in the SI, found no fundamental change in the mechanism.

The results presented here have a number of implications. Perhaps the most obvious is, at least for the conditions considered, the inevitability of peptide adsorption for solid surfaces that interact strongly with the solution phase. This inevitability has its origins in the existence of the water layers adjacent to the solid surface. First, the effective charged layering

at the surface arises from orientational structuring of the interfacial water greatly extends the surface's influence into the solution phase, enhancing the draw-down of peptides toward it. Second, once near the interface, a peptide is easily anchored for long periods through relatively strong interactions between its hydrophilic parts and the water layers, allowing it time to rearrange and fully adsorb. Finally, while the water layer immediately adjacent to the solid surface slows the adsorption process due to its tightly bound nature, its charged and highly hydrophilic nature means it strongly binds a peptide once adsorption begins.

The findings here also suggest a number of conditions under which peptide adsorption may be mitigated for 'strongly interacting' uncharged surfaces. Fluid flow would tend to counteract the biased diffusion, reducing the flux of peptides to the surface. Flow-induced shear at the interface would also enhance peptide de-anchoring before lock-down can start. Peptides dominated by hydrophobic residues such as polyalanines would tend to be poorer adsorbers because both the driving force for biased diffusion will be low and only their charged termini would in general act as effective anchors (i.e., allow sufficient time for lockdown to initiate). Finally, as both we and Yu et al.[48] have observed that internal rearrangement of the peptide makes for a more effective lock-down process, it is possible that proteins that are unable to easily undergo such rearrangement may not be strong adsorbers, a possibility that has long been supported by experiment[16] (this is not to say that adsorption is not possible for rigid peptides but, as suggested by the work of Hoefling et al.[47] on a relatively rigid β-sheet peptide, it is likely that it will take longer as rigid body motion will be necessary).

The results here also have possible implications for MD-based efforts to determine the free energy of adsorption of peptides on strongly interacting solid surfaces such as those of metals. First, the strong binding that occurs between the solution phase and the surface implies that adequate sampling by the peptide of its phase space will be extremely difficult to achieve when it is close to the surface. There are methods that in principle may allow this issue to be overcome. One is to adopt thermal-based replica exchange MD. However, our initial work (unpublished) suggests that this alone is not only expensive but also does not lead to particularly good results at least when used in conjunction with thermodynamic integration. An alternative is to use a biasing approach such as that adopted by O'Brien et al.[58] However, this approach would counter the strong role played by the water layers, which would be captured in the potential of mean force used to apply biasing, destroying the basis for the adsorption mechanism seen here. An alternative enhanced sampling approach that may be more appropriate, however, is replica exchange with solute tempering, as it appears to allow preservation of water layering at the solid interface.[59]

■ CONCLUSIONS

By interrogating the results of over 240 MD simulations, we have been able to draw general conclusions about the mechanism for peptide adsorption from the bulk solution phase on to 'strongly interacting' solid surfaces such as those of metals. The mechanism is composed of three phases as illustrated by Figure 1: (1) biased diffusion of the peptide from the bulk phase toward the water/solid interface; (2) anchoring of the peptide to the interface either via hydrogen bonding between one of its hydrophilic groups and the second of two

strong water layers that exist at the interface, or strong interaction arising between a sulfur- or benzyl-containing side chain and the underlying solid surface; and (3) a slow, stepwise lockdown of the peptide directly onto the surface where the groups generally follow the initial group in a sequential fashion (termed statistical zippering) as they fill adjacent fleeting voids that occur intermittently in the strongly bound water layer immediately next to the surface.

The observed adsorption mechanism is critically dictated by the presence of two strong water layers at the water/solid interface and their orientational ordering. Most obviously, these layers effectively project the solid surface around 8 Å into the fluid. However, of particular note is their inducing of charged layers at the interface, which arise from the orientational ordering that (1) bring into play long-range electrostatic interaction between the interface and the peptide that enhances diffusion of the latter toward the surface and (2) facilitates relatively strong anchoring of the peptide at the interface so as to allow sufficient time for it to rearrange and start displacing the tightly bound first water layer and adsorb directly onto the solid surface.

The mechanism reported here has support from both the very limited experimental data as well as other MD-based studies, and it also offers up insight into observations made in both bodies of literature (e.g., why peptide flexibility is important to full adsorption) that have until now gone unexplained as well as wholly new insights (e.g., the origins of the biased diffusion phase; anchoring and its importance). Given this and the fact that the results obtained for the two very different peptide sequences considered here are qualitatively very similar, we believe the proposed adsorption mechanism is quite general for the conditions considered. Furthermore, if one considers proteins as an assembly of peptides, the work reported here is also relevant to adsorption of proteins under these conditions. Finally, the results here also allow conjectures to be drawn for conditions beyond this, including for protein adsorption when fluid flow is present and when it is internally rigid (i.e., 'hard' in Norde's[16] parlance).

Surfaces that interact more weakly with the solution phase, such as graphite/graphene and self-assembled monolayers, are clearly of interest. So too is the situation where the peptide/protein solution phase is nondilute. We are, thus, bringing the same approach used here—statistical analysis of results from a large number of simulations of the same system—to elucidate the adsorption mechanism for these and other cases. Results of these studies will appear in future reports.

ASSOCIATED CONTENT

S **Supporting Information**

(1) Method in detail. (2) Signposted movie of the trajectory in Figure 2. (3) Quantitative analysis of the biased diffusion. (4) Water density analysis around the SD152 peptide. (5) Distribution of lockdown times for the A3 peptide. (6) Further support for the zippering process that underpins lockdown. (7) Diffusion analysis. (8) Comparison of results obtained for the A3 peptide on a Lennard-Jones and polarizable gold surface. This material is available free of charge via the Internet at http://pubs.acs.org.

AUTHOR INFORMATION

Corresponding Author
mark.biggs@adelaide.edu.au

Notes
The authors declare no competing financial interest.

REFERENCES

(1) Hoang, Q. Q.; Sicheri, F.; Howard, A. J.; Yang, D. S. C. *Nature* **2003**, *425*, 977.
(2) Hartgerink, J. D.; Beniash, E.; Stupp, S. I. *Science* **2001**, *294*, 1684.
(3) Pouget, E.; Dujardin, E.; Cavalier, A.; Moreac, A.; Valéry, C.; Marchi-Artzner, V.; Weiss, T.; Renault, A.; Paternostre, M.; Artzner, F. *Nat. Mater.* **2007**, *6*, 434.
(4) Nel, A. E.; Madler, L.; Velegol, D.; Xia, T.; Hoek, E. M. V.; Somasundaran, P.; Klaessig, F.; Castranova, V.; Thompson, M. *Nat. Mater.* **2009**, *8*, 543.
(5) Choi, H. S.; Liu, W.; Liu, F.; Nasr, K.; Misra, P.; Bawendi, M. G.; Frangioni, J. V. *Nat. Nanotechnol.* **2010**, *5*, 42.
(6) Cho, N.-H.; Cheong, T.-C.; Min, J. H.; Wu, J. H.; Lee, S. J.; Kim, D.; Yang, J.-S.; Kim, S.; Kim, Y. K.; Seong, S.-Y. *Nat. Nanotechnol.* **2011**, *6*, 675.
(7) Dankers, P. Y. W.; Harmsen, M. C.; Brouwer, L. A.; Van Luyn, M. J. A.; Meijer, E. W. *Nat. Mater.* **2005**, *4*, 568.
(8) Niemeyer, C. M. *Angew. Chem., Int. Ed.* **2001**, *40*, 4128.
(9) Sarikaya, M.; Tamerler, C.; Jen, A. K. Y.; Schulten, K.; Baneyx, F. *Nat. Mater.* **2003**, *2*, 577.
(10) Im, H.; Huang, X.-J.; Gu, B.; Choi, Y.-K. *Nat. Nanotechnol.* **2007**, *2*, 430.
(11) Fischer, T.; Agarwal, A.; Hess, H. *Nat. Nanotechnol.* **2009**, *4*, 162.
(12) Orosco, M. M.; Pacholski, C.; Sailor, M. J. *Nat. Nanotechnol.* **2009**, *4*, 255.
(13) Thingholm, T. E.; Jorgensen, T. J. D.; Jensen, O. N.; Larsen, M. R. *Nat. Protoc.* **2006**, *1*, 1929.
(14) Gräslund, S.; Nordlund, P.; Weigelt, J.; Hallberg, B. M.; Bray, J.; Gileadi, O.; Knapp, S.; Oppermann, U.; Arrowsmith, C.; Hui, R.; Ming, J.; dhe-Paganon, S.; Park, H.; Savchenko, A.; Yee, A.; Edwards, A.; Vincentelli, R.; Cambillau, C.; Kim, R.; Kim, S.-H.; Rao, Z.; Shi, Y.; Terwilliger, T. C.; Kim, C.-Y.; Hung, L.-W.; Waldo, G. S.; Peleg, Y.; Albeck, S.; Unger, T.; Dym, O.; Prilusky, J.; Sussman, J. L.; Stevens, R. C.; Lesley, S. A.; Wilson, I. A.; Joachimiak, A.; Collart, F.; Dementieva, I.; Donnelly, M. I.; Eschenfeldt, W. H.; Kim, Y.; Stols, L.; Wu, R.; Zhou, M.; Burley, S. K.; Emtage, J. S.; Sauder, J. M.; Thompson, D.; Bain, K.; Luz, J.; Gheyi, T.; Zhang, F.; Atwell, S.; Almo, S. C.; Bonanno, J. B.; Fiser, A.; Swaminathan, S.; Studier, F. W.; Chance, M. R.; Sali, A.; Acton, T. B.; Xiao, R.; Zhao, L.; Ma, L. C.; Hunt, J. F.; Tong, L.; Cunningham, K.; Inouye, M.; Anderson, S.; Janjua, H.; Shastry, R.; Ho, C. K.; Wang, D.; Wang, H.; Jiang, M.; Montelione, G. T.; Stuart, D. I.; Owens, R. J.; Daenke, S.; Schütz, A.; Heinemann, U.; Yokoyama, S.; Büssow, K.; Gunsalus, K. C. *Nat. Methods* **2008**, *5*, 135.
(15) Vroman, L. *Nature* **1962**, *196*, 476.
(16) Norde, W. *Colloids. Surf. B: Biointerfaces* **2008**, *61*, 1.
(17) Norde, W. *Adv. Colloid Interface Sci.* **1986**, *25*, 267.
(18) Mermut, O.; Phillips, D. C.; York, R. L.; McCrea, K. R.; Ward, R. S.; Somorjai, G. A. *J. Am. Chem. Soc.* **2006**, *128*, 3598.
(19) Li, Q.; Lau, K. H. A.; Sinner, E. K.; Kim, D. H.; Knoll, W. *Langmuir* **2009**, *25*, 12144.
(20) Rabe, M.; Verdes, D.; Seeger, S. *Adv. Colloid Interface Sci.* **2011**, *162*, 87.
(21) Morra, M. *J. Biomater. Sci., Polym. Ed* **2000**, *11*, 547.
(22) Chen, H.; Yuan, L.; Song, W.; Wu, Z.; Li, D. *Prog. Polym. Sci.* **2008**, *33*, 1059.

(23) Jeon, S. I.; Lee, J. H.; Andrade, J. D.; De Gennes, P. G. *J. Colloid Interface Sci.* **1991**, *142*, 159.

(24) Szleifer, I. *Biophys. J.* **1997**, *72*, 595.

(25) Wang, R. L. C.; Kreuzer, H. J.; Grunze, M. *J. Phys. Chem. B* **1997**, *101*, 9767.

(26) Harder, P.; Grunze, M.; Dahint, R.; Wjitesides, G. M.; Laibinis, P. E. *J. Phys. Chem. B* **1998**, *102*, 426.

(27) Li, L.; Chen, S.; Zheng, J.; Ratner, B. D.; Jiang, S. *J. Phys. Chem. B* **2005**, *109*, 2934.

(28) Pasche, S.; Vörös, J.; Griesser, H. J.; Spencer, N. D.; Textor, M. *J. Phys. Chem. B* **2005**, *109*, 17545.

(29) Duff, M. R., Jr; Kumar, C. V. *J. Phys. Chem. B* **2009**, *113*, 15083.

(30) Pinholt, C.; Hartvig, R. A.; Medlicott, N. J.; Jorgensen, L. *Expert Opin. Drug Delivery* **2011**, *8*, 949.

(31) Gray, J. J. *Curr. Opin. Struct. Biol.* **2004**, *14*, 110.

(32) Fenoglio, I.; Fubini, B.; Ghibaudi, E. M.; Turci, F. *Adv. Drug Delivery Rev.* **2011**, *63*, 1186.

(33) Braun, R.; Sarikaya, M.; Schulten, K. S. *J. Biomater. Sci.* **2002**, *13*, 747.

(34) Song, D.; Forciniti, D. *J. Chem. Phys.* **2002**, *115*, 8089.

(35) Mungikar, A. A.; Forciniti, D. *Biomacromolecules* **2004**, *5*, 2147.

(36) Oren, E. E.; Tamerler, C.; Sarikaya, M. *Nano Lett.* **2005**, *5*, 415.

(37) Raut, V. P.; Agashe, M. A.; Stuart, S. J.; Latour, R. A. *Langmuir* **2005**, *21*, 1629.

(38) Monti, S. *J. Phys. Chem. C* **2007**, *111*, 6086.

(39) Skelton, A. A.; Laing, T.; Walsh, T. R. *ACS Appl. Mater. Interfaces* **2009**, *1*, 1482.

(40) Heinz, H.; Farmer, B. L.; Pandey, R. B.; Slocik, J. M.; Patnaik, S. S.; Pachter, R.; Naik, R. R. *J. Am. Chem. Soc.* **2009**, *131*, 9704.

(41) Verde, A. V.; Acres, J. M.; Maranas, J. K. *Biomacromolecules* **2009**, *10*, 2118.

(42) Raffaini, G.; Ganazzoli, F. *Langmuir* **2010**, *26*, 5679.

(43) Oren, E. E.; Notman, R.; Kim, I. W.; Evans, J. S.; Walsh, T. R.; Tamerler, C.; Sarikaya, M. *Langmuir* **2010**, *26*, 11003.

(44) Penna, M. J.; Biggs, M. J. *The Binding Mechanism of an Experimentally Identified Platinum-binding Peptide by Molecular Dynamics Simulation*, In Chemeca 2010: Engineering at the Edge, Hilton Adelaide, South Australia, September 26-29, 2010; Barton, A.C.T.: Australia, 2010; 289−298.

(45) Verde, A. V.; Beltramo, P. J.; Maranas, J. K. *Langmuir* **2011**, *27*, 5918.

(46) Patwardhan, S. V.; Emami, F. S.; Berry, R. J.; Jones, S. E.; Naik, R .R.; Deschaume, O.; Heinz, H.; Perry, C. C. *J. Am. Chem. Soc.* **2012**, *134*, 6244.

(47) Hoefling, M.; Monti, S.; Corni, S.; Gottschalk, K. E. *PLoS ONE* **2011**, *6*, e20925.

(48) Yu, J.; Becker, M. L.; Carri, G. A. *Langmuir* **2012**, *28*, 1408.

(49) The mapping of the phases of Penna and Biggs[44] to the regimes of Yu and co-workers[48] are as follows: biased-diffusion phase + anchoring phase = diffusive regime; initiation of the lockdown phase = anchoring regime; lockdown phase = crawling regime + binding regime.

(50) Seker, U. O. S.; Wilson, B.; Dincer, S.; Kim, I. W.; Oren, E. E.; Evans, J. S.; Tamerler, C.; Sarikaya, M. *Langmuir* **2007**, *23*, 7895.

(51) Seker, U. O. S.; Wilson, B.; Sahin, D.; Tamerler, C.; Sarikaya, M. *Biomacromolecules* **2009**, *10*, 250.

(52) Slocik, J. M.; Stone, M. O.; Naik, R. R. *Small* **2005**, *1*, 1048.

(53) Amino acid code meaning: A = Ala = alanine; C = Cys = cysteine; F = Phe = phenylalanine; G = Gly = glycine; M = Met = Methionine; P = Pro = proline; Q = Gln = glutamine; S = Ser = serine; T = Thr = threonine; Y = Try = tyrosine.

(54) A hydrophilic group is deemed to have 'accompanied' a nonpolar anchor if it enters the second water layer within no more than 100 ps of the anchoring occurring. This period is based on a conservative estimate of the time that elapses between a hydrophilic group forming a 'strong' interaction (e.g., hydrogen bond) with the second water layer and it directly entering the water layer (i.e., it reflects the assertion that when a hydrophilic group accompanies a nonpolar anchor, it is likely that the hydrophilic group is playing a major role in the anchoring).

(55) Schravendijk, P.; Ghiringhelli, L. M.; Site, L. D.; van der Vegt, N. F. A. *J. Phys. Chem. C* **2007**, *111*, 2631.

(56) Iori, F.; Corni, S. *J. Comput. Chem.* **2008**, *29*, 1656.

(57) Iori, F.; Di Felice, R.; Molinari, E.; Corni, S. *J. Comput. Chem.* **2009**, *30*, 1465.

(58) O'Brien, C. P.; Stuart, S. J.; Bruce, D. A.; Latour, R. A. *Langmuir* **2008**, *24*, 14115.

(59) Wright, L. B.; Walsh, T. R. *Phys. Chem. Chem. Phys.* **2013**, *15*, 4715.